

NACA RM L51J17

APR 17 1952
UNCLASSIFIED

NACA

RESEARCH MEMORANDUM

FREE-FLIGHT INVESTIGATION OF LONGITUDINAL STABILITY

AND CONTROL OF A ROCKET-PROPELLED MISSILE

MODEL HAVING CRUCIFORM, TRIANGULAR,
INLINE WINGS AND TAILS

By James R. Hall

Langley Aeronautical Laboratory
Langley Field, Va.

CLASSIFIED DOCUMENT

This material contains information affecting the National Defense of the United States within the meaning of the espionage laws, Title 18, U.S.C., Secs. 793 and 794, the transmission or revelation of which in any manner to unauthorized person is prohibited by law.

NATIONAL ADVISORY COMMITTEE FOR AERONAUTICS

WASHINGTON
March 25, 1952

NACA LIBRARY
LANGLEY AERONAUTICAL LABORATORY
Langley Field, Va.

UNCLASSIFIED

CLASSIFIED BY NACM

UNCLASSIFIED

Authority of
DHS A
2/20/14

2-19-68

Authority of

UNCLASSIFIED

CLASSIFICATION CHANGED

to
Many to do Adg... 888 Oct 19 1967
Dep... 11-2-68

1-24-68

UNCLASSIFIED

1M

NACA RM L51J17

NATIONAL ADVISORY COMMITTEE FOR AERONAUTICS

RESEARCH MEMORANDUM

FREE-FLIGHT INVESTIGATION OF LONGITUDINAL STABILITY

AND CONTROL OF A ROCKET-PROPELLED MISSILE

MODEL HAVING CRUCIFORM, TRIANGULAR,

INLINE WINGS AND TAILS

By James R. Hall

SUMMARY

A rocket-propelled missile model having cruciform, triangular, inline wings and tails has been flight-tested through the Mach number range of 0.65 to 1.55 at small wing-deflection angles. The Reynolds number, based on the mean aerodynamic chord, varied from 5.7×10^6 at Mach number 0.65 to 17×10^6 at Mach number 1.55. The results are presented and compared with results from a previously flown model having interdigitated tails. The static stability of the inline configuration is less than for the interdigitated, particularly above Mach number 1.25 and through the transonic range. The damping factor is quite similar for both configurations. Control effectiveness is considerably greater for the inline configuration, the greatest increase occurring through the transonic range. Trim normal-force coefficient per unit wing-deflection angle for the inline configuration is about three times as large as that for the interdigitated model. The hinge moments measured for the interdigitated configuration were substantiated by the data for the inline configuration.

INTRODUCTION

As part of a flight-test program being conducted by the Langley Pilotless Aircraft Research Division of the NACA on missiles having cruciform, triangular wings and tails, a second dynamic model has been flight-tested. The horizontal wings of the model were controllable in a square-wave pattern to induce pitching oscillations from which longitudinal stability and control characteristics were obtained. The present model was identical to the first, reported in reference 1, except that the tail fins were oriented in line with the wings instead of being interdigitated.

CLASSIFICATION CHANGED

UNCLASSIFIED

CLASSIFICATION CHANGED

UNCLASSIFIED

Handwritten notes:
 Langley (Langley) 2250 Oct 19 1967 (Classified)
 Static stability and control characteristics (Classified)
 Authority of Langley (Langley) 1-24-68
 Date

Handwritten notes:
 Encl
 1-24-68

Handwritten notes:
 DASA
 CD 143

Handwritten notes:
 8-14-68

UNCLASSIFIED

SYMBOLS

C_N	normal-force coefficient assumed equal to lift coefficient for small angles of attack $\left(\frac{\text{Normal force}}{qS} \right)$
C_m	pitching-moment coefficient $\left(\frac{\text{Pitching moment}}{qS\bar{c}} \right)$
C_h	hinge-moment coefficient $\left(\frac{\text{Hinge moment}}{qS\bar{c}} \right)$
I	moment of inertia in pitch, slug-feet ²
q	dynamic pressure, pounds per square foot
S	exposed area of two wing panels, 3.21 square feet
\bar{c}	mean aerodynamic chord of exposed wing, 1.572 feet
c_r	wing chord at wing-fuselage juncture
α	angle of attack, degrees
θ	angle of pitch, degrees
δ	wing-deflection angle, positive when leading edge is up, degrees
m	mass of model, slugs
M	Mach number
V	velocity, feet per second
P	period of short-period longitudinal oscillation, seconds
$T_{1/2}$	time to damp oscillation to one-half amplitude, seconds
$C_{m_q} + C_{m_{\dot{\alpha}}}$	damping factor

Subscripts:

$$\dot{\alpha} = \frac{d\alpha}{dt} \frac{\bar{c}}{2V}$$

$$q = \frac{d\theta}{dt} \frac{\bar{c}}{2V}$$

Subscripts used with coefficients indicate partial derivatives. All angles are in degrees and angular velocities are in degrees per second.

MODELS AND TEST PROCEDURE

A photograph of the subject model is given in figure 1. Dimensions of the model are given in figure 2. The model was identical to the interdigitated configuration reported in reference 1 except for the inline tails.

Dural construction was used throughout, except for the brass nose. The fuselage was formed of 0.064-inch-thick 75S-T dural skin stiffened with bulkheads and strengthened with a heavy forged center-body and tail section of 24S-T dural. The wings and tails were forged and machined, respectively, of 24S-T dural. The model was ballasted to have the same center-of-gravity location as the interdigitated model.

Originally intended for a zero-lift drag investigation, the models were adapted by the NACA to accommodate a wing-pulsing mechanism in order to obtain data on the dynamic characteristics of the model. The wing-deflection angles employed in the tests were limited to small values owing to structural limitations of the models. The wing-deflection angle of the current model varied between $\pm 0.8^\circ$ at Mach number 1.5 and $\pm 1.2^\circ$ at Mach number 0.65. For the previously reported interdigitated model, the wing deflection varied between $\pm 1.5^\circ$ at Mach number 1.5 and $\pm 1.8^\circ$ at Mach number 0.75. The physical characteristics of both models are given in table I.

The model was launched from a rail launcher at an elevation of 50° . It was boosted by an ABL Deacon rocket motor of 19,800 pound-seconds impulse to a Mach number of about 1.0, whereupon the model separated from the booster and the internal rocket motor of 7200 pound-seconds impulse accelerated it to a Mach number 1.55.

Doppler radar provided a velocity history of the model for the first 10 seconds of the flight, whereafter velocity was obtained from the ratio of the total pressure to the static pressure. Static pressure throughout the flight was obtained from radiosonde measurements in conjunction with displacement radar measurements of the flight path. The model was equipped with an NACA eight-channel telemeter. Measurements

~~CONFIDENTIAL~~

were made of normal, transverse, and longitudinal acceleration of the angle of attack, hinge moment, wing-deflection angle, total pressure, and static pressure.

The method of reducing the telemeter data is reported in detail in reference 2. Briefly, the telemeter data were recorded in the form of time histories of a series of damped oscillations from which measurements were made of the aerodynamic quantities. The period P of the oscillations was obtained directly from the record. The time to damp to one-half amplitude was obtained analytically from the rate of decay of the short-period oscillation. The static stability derivative C_{m_α} and the damping factor $C_{m_q} + C_{m_{\dot{\alpha}}}$ were obtained considering two degrees of freedom by the following relationships:

$$C_{m_\alpha} = \frac{I}{qS\bar{c}} \left[\frac{4\pi^2}{p^2} + \left(\frac{0.693}{T_{1/2}} \right)^2 \right] \quad (1)$$

$$C_{m_q} + C_{m_{\dot{\alpha}}} = \frac{2}{57.3} \frac{I}{mc^2} \left[C_{L_\alpha} - \frac{1.386}{T_{1/2}} \frac{mV}{qS} \right] \quad (2)$$

The value of $(\alpha/\delta)_{trim}$ was obtained from the measured trim values of α and δ . The equation $-\frac{C_{m_\delta}}{C_{m_\alpha}} = \left(\frac{\alpha}{\delta} \right)_{trim}$ was used to evaluate C_{m_δ} . Trim normal-force coefficient per wing-deflection angle $(C_{N_\delta})_{trim}$ was obtained using the increment in the trim values of $C_{N_{trim}}$ between successive values of δ_{trim} .

RESULTS AND DISCUSSION

The aerodynamic information provided by the flight test of the subject test vehicle is presented in figures 3 to 9. Comparative curves for the interdigitated model previously flown and wind-tunnel test points

~~CONFIDENTIAL~~

transferred to the center of gravity of the flight models are also given whenever possible. The Reynolds number, based on the mean aerodynamic chord, varied from 5.7×10^6 at Mach number 0.65 to 17×10^6 at Mach number 1.55. The telemeter functioned continuously for the duration of the flight, but an unexplainable sudden shift in the angle-of-attack record during internal rocket firing affected the usefulness of subsequent angle-of-attack data during periods of rapidly changing angle of attack. Trim values of angle of attack were satisfactorily recorded however. As a consequence, direct determination of the lift-curve slope C_{L_α} was not possible. A method was devised to verify the hinge-moment derivatives of the previous flight on the basis of the limited angle of attack information available and the previously measured values of C_{h_α} and C_{h_δ} .

The method is discussed under the section entitled "Hinge Moments." The method is not applicable to substantiation of normal-force derivatives because unlike hinge-moment derivatives, they are different for the inline and interdigitated cases.

Stability and Damping

The variation of the period P of the short-period oscillation and the time to damp to one-half amplitude $T_{1/2}$ with Mach number are shown in figure 3. It should be noted that these values are associated with the particular conditions prevailing during the flight of the subject model. The variation of static stability C_{m_α} with Mach number, calculated from the foregoing values of period and time to damp to one-half amplitude for an average wing-deflection angle of 1.1° , is shown in figure 4. In both models the center of gravity was located at 50.8 percent of the mean aerodynamic chord. The inline configuration was stable throughout the Mach number range, although less stable than the interdigitated configuration, particularly above Mach number 1.25 and in the transonic range. Wind-tunnel test points (references 3 and 4) shown at Mach numbers 1.5, 0.9, and 0.7 for $\alpha = \delta = 0^\circ$ also indicate a loss of stability for the inline configuration, particularly at subsonic Mach numbers.

The wind-tunnel results of reference 4 and the flight-test results of reference 5 indicate an appreciable increase in the supersonic static stability for the inline configuration when trimmed with the wing deflected over that obtained with the wing undeflected. The 4° change of wing-deflection angle reported in reference 4 changed C_{m_α} at α_{trim} from -0.019 at $\delta = 0^\circ$ to -0.076 at $\delta = 4^\circ$. Even the small wing-deflection angle of 1.5° was enough to double the static stability of the flight test model reported in reference 5. Linear interpolation of the wind-tunnel test points for a wing-deflection angle of 1.5° gives a value

of $C_{m\alpha}$ very close to that reported for the flight test of reference 5. Quantitative wind-tunnel information at subsonic speeds is not available at appropriate angles of attack and wing deflections other than zero, although, as indicated above, such information should give better agreement between the static stability reported by wind tunnel and the subject flight test. Aeroelastic effects of the tail would be expected to cause lower flight test values of $C_{m\alpha}$ because of the higher dynamic pressure of the flight tests.

The variation of the damping factor $C_{m_q} + C_{m\dot{\alpha}}$ with Mach number is shown in figure 5. Equation (2) was used to obtain $C_{m_q} + C_{m\dot{\alpha}}$. In the absence of flight-test values of $C_{L\alpha}$ for the inline configuration, the previously determined flight-test values for the interdigitated tail configuration were used. Since there are indications (references 3 and 4) that the subsonic and transonic lift-curve slopes are greater for the interdigitated than for the inline configuration, the values of $C_{m_q} + C_{m\dot{\alpha}}$ as determined from the present tests may be somewhat conservative. Damping is maintained throughout the test Mach number range. Like the interdigitated configuration, the inline configuration exhibits less damping at supersonic than at subsonic Mach numbers and a peak at transonic Mach numbers. The increase in damping of the inline configuration at Mach number 1.35 reflects the decreased time to damp shown in figure 3.

Control Effectiveness

The variation of control effectiveness as measured by the parameters $C_{m\delta}$ and $(\alpha/\delta)_{trim}$ is shown in figures 6 and 7. Both configurations maintained control effectiveness throughout the Mach number range but displayed decreasing control effectiveness above the transonic range. The parameter $(\alpha/\delta)_{trim}$ for the inline configuration is considerably larger than for the interdigitated configuration owing largely to increased

$C_{m\delta}$. The equation $-\frac{C_{m\delta}}{C_{m\alpha}} = \left(\frac{\alpha}{\delta}\right)_{trim}$ which relates the two parameters

indicates their interdependence. It can be seen that the decreased static stability of the inline configuration also contributes to the increased $(\alpha/\delta)_{trim}$. In the test vehicle, $C_{m\delta}$ for this center-of-gravity location is due almost entirely to tail lift created by downwash from the deflected wing. Hence, any variation in the downwash pattern would have a strong effect on $C_{m\delta}$. Therein lies a partial explanation of the greater control effectiveness of the inline configuration. For the small wing deflections employed it was possible for the main downwash disturbance to pass

between the interdigitated fins having little effect on $C_{m\delta}$, whereas the inline configuration would be sensitive to the downwash even at low wing-deflection angles. Wind-tunnel values of $(\alpha/\delta)_{trim}$ and $C_{m\delta}$ transferred to the center of gravity of the test models are given in the figures. All wind-tunnel data were based on 4° wing deflection while the flight test wing-deflection angles averaged 1.60° for the interdigitated case and 1.10° for the inline configuration. The larger values of $C_{m\delta}$ of the wind-tunnel results over flight-test results for the interdigitated configuration tend to substantiate the foregoing explanation of tail effectiveness. For the inline configuration, the wind-tunnel values of $C_{m\delta}$ agreed very well with flight-test results at Mach number 1.5 but were low at subsonic Mach numbers. Wind-tunnel values of $(\alpha/\delta)_{trim}$ at Mach number 1.5 were higher than flight-test results for both configurations, but were indicative of the much higher control effectiveness of the inline configuration. At subsonic speeds the wind-tunnel data indicated very high values of $(\alpha/\delta)_{trim}$ for the inline configuration owing to the low static stability. The variation of $(C_{N\delta})_{trim}$ with Mach number is shown in figure 8. The higher control effectiveness of the inline configuration is indicated by a 300-percent increase in $(C_{N\delta})_{trim}$ with the characteristic increase through the transonic range.

Hinge Moments

Direct determination of $C_{h\alpha}$ and $C_{h\delta}$ was not possible for the subject model without complete angle-of-attack information; however, an indirect method was devised. The equation $C_{h_{trim}} = \alpha_{trim}C_{h\alpha} + \delta_{trim}C_{h\delta}$ was solved using the measured α_{trim} and δ_{trim} and the previously determined values (reference 1) of $C_{h\alpha}$ and $C_{h\delta}$. The result was then compared with the measured value of $C_{h_{trim}}$ giving excellent agreement and substantiating the validity of the component data. Figure 9 shows the hinge-moment derivatives from reference 1 which were used in the calculations. Also shown are the measured and predicted values of $(C_h)_{trim}$ indicating the excellent agreement obtained.

CONCLUSIONS

Flight tests at low wing-deflection angles of the tail inline configuration of the test missile indicate less static stability than for the interdigitated configuration, particularly above Mach number 1.25 and at transonic Mach numbers. The damping factor $C_{m_q} + C_{m_{\dot{\alpha}}}$ is similar for both configurations, the inline configuration exhibiting slightly lower damping below Mach number 1.35. Control effectiveness indicated by the parameters $C_{m_{\delta}}$ and $(\alpha/\delta)_{trim}$ is considerably greater for the inline than for the interdigitated configuration. A marked increase in effectiveness occurs through the transonic range for the inline configuration. Trim normal-force coefficient per unit wing-deflection angle for the inline configuration is about three times as large as for the interdigitated model with the characteristic increase through the transonic range. The hinge-moment derivatives for the inline case were the same as for the interdigitated case.

Langley Aeronautical Laboratory
National Advisory Committee for Aeronautics
Langley Field, Va.

REFERENCES

1. Sandahl, Carl A., and Hall, James R.: Free-Flight Investigation of the Longitudinal Stability and Control of a Rocket-Propelled Missile Model Having Cruciform, Triangular, Interdigitated Wings and Tails. NACA RM L51B15, 1951.
2. Gillis, Clarence L., Peck, Robert F., and Vitale, A. James: Preliminary Results from a Free-Flight Investigation at Transonic and Supersonic Speeds of the Longitudinal Stability and Control Characteristics of an Airplane Configuration with a Thin Straight Wing of Aspect Ratio 3. NACA RM L9K25a, 1950.
3. Magnus, R. J., Beal, R. R., and Kutschinski, C. R.: Sparrow 13-D. Analysis of Force and Moment Characteristics from Subsonic Wind-Tunnel Tests of a 50-Percent-Scale Model. Rep. No. SM-13632, Douglas Aircraft Co., Inc., March 15, 1950.
4. Sager, B. F., Kutschinski, C. R., and Goldbaum, G. C.: Sparrow 13-D. Analysis of Force and Moment Characteristics from Supersonic Wind-Tunnel Tests of a 13.5-Percent-Scale Model. Rep. No. SM-13631, Douglas Aircraft Co., Inc., March 17, 1950.
5. Kutschinski, C. R.: Preliminary Analysis of Aerodynamic Data from Pitch Program-Controlled Sparrow 13-E Missile Flight 0052. Rep. No. SM-13800, Douglas Aircraft Co., Inc., Nov. 3, 1950.

TABLE I

PHYSICAL CHARACTERISTICS OF INLINE AND INTERDIGITATED CONFIGURATIONS

	Inline subject model	Interdigitated (reference 1)
Weight, lb:		
Loaded	333.5	342
Internal rocket motor expended	292.5	301
Center-of-gravity location, station:		
Loaded	75.7	75.8
Internal rocket motor expended	71.3	71.3
Center-of-gravity location, percent M.A.C.:		
Loaded	74.4	74.9
Internal rocket motor expended	50.8	50.8
Moment of inertia in pitch, sustainer motor expended, slug-ft ²		
	107.2	112.0
Wing hinge line, percent M.A.C. exposed wing . .	43	43
Wing panel area, exposed, sq ft	1.605	1.605
Tail panel area, exposed, sq ft	0.637	0.637
Mean aerodynamic chord of exposed wing panel, ft		
	1.572	1.572
Wing thickness ratio	0.04	0.04
Tail thickness ratio	0.03	0.03
Wing-deflection angle, deg	±0.8 to ±1.2	±1.5 to ±1.8



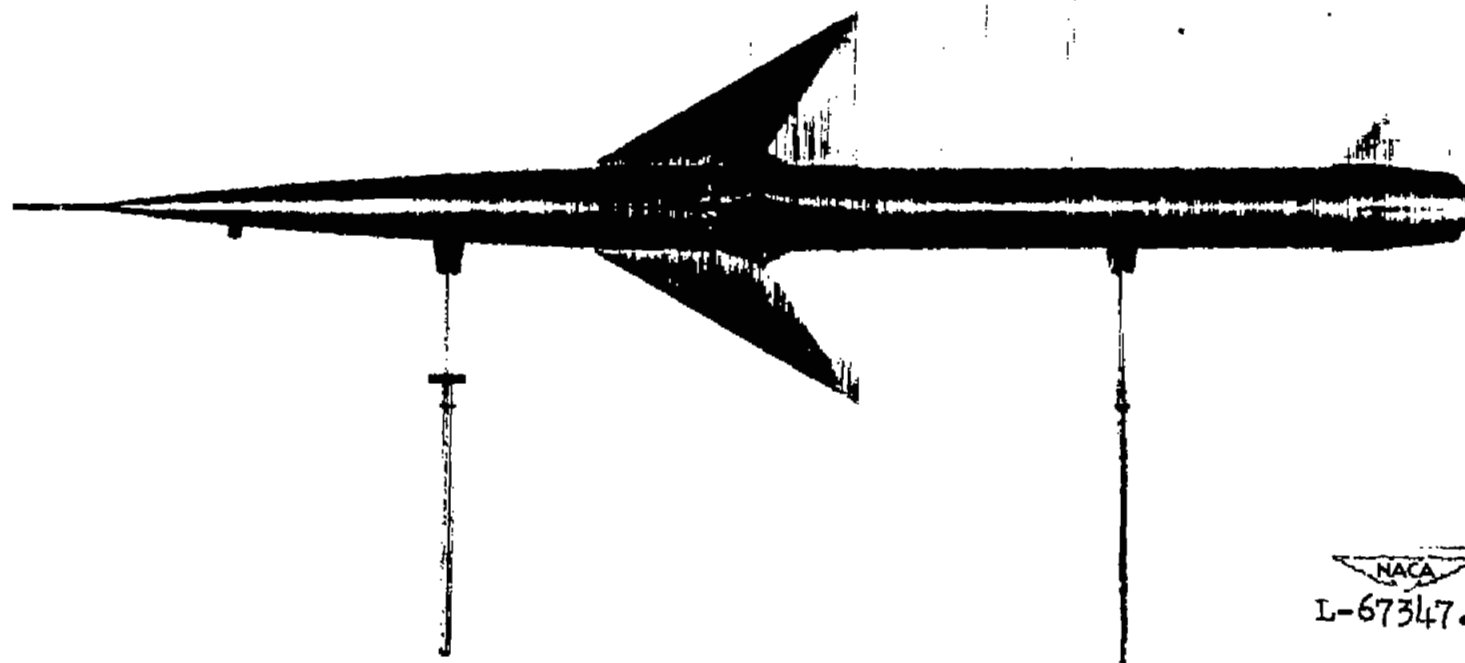


Figure 1.- Photograph of subject model.

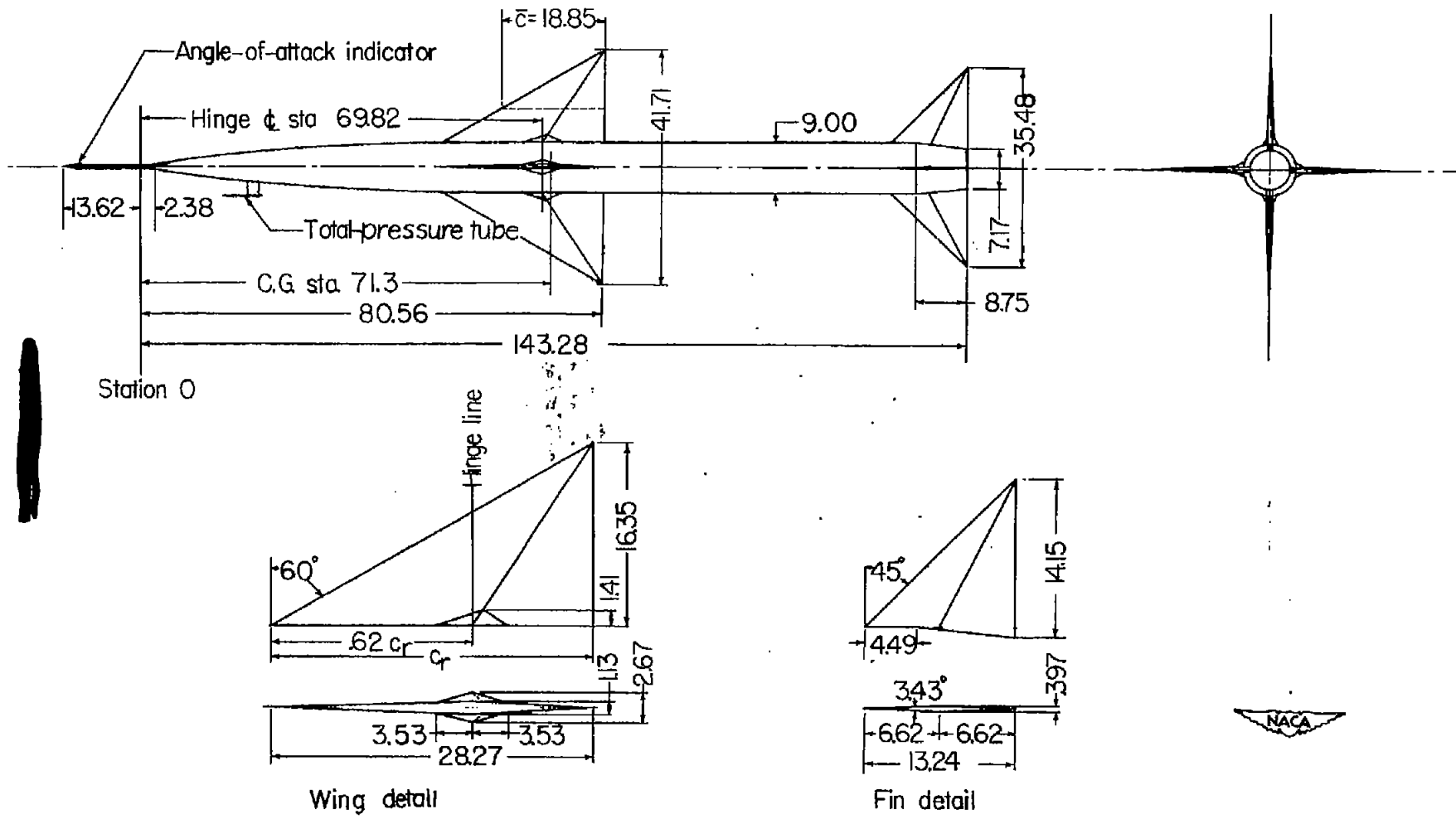


Figure 2.- General arrangement of test vehicle. All dimensions are in inches.

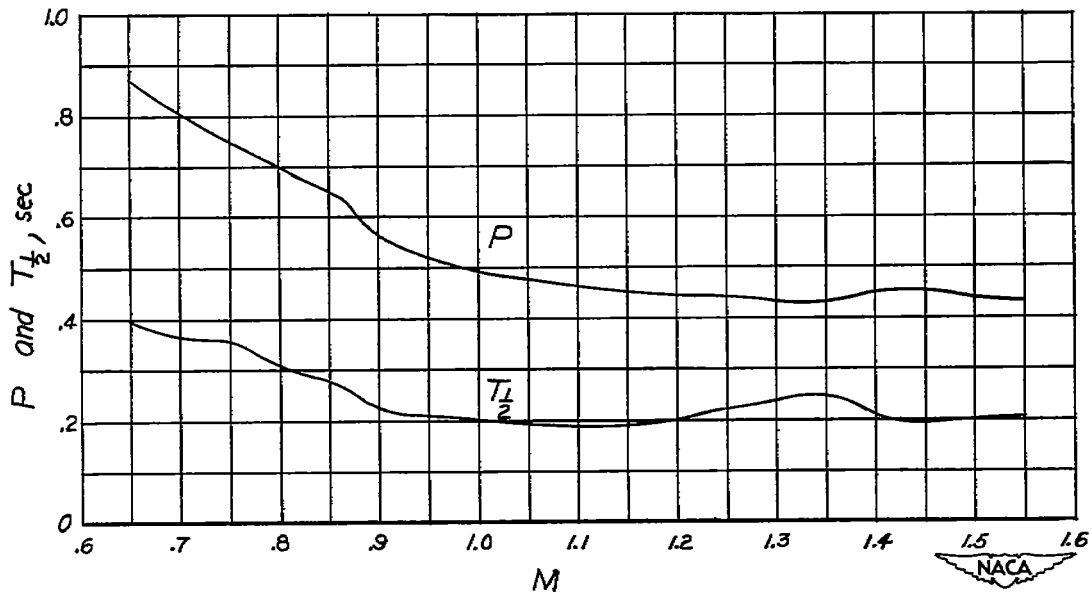


Figure 3.- Variation of period and time to damp to one-half amplitude with Mach number.

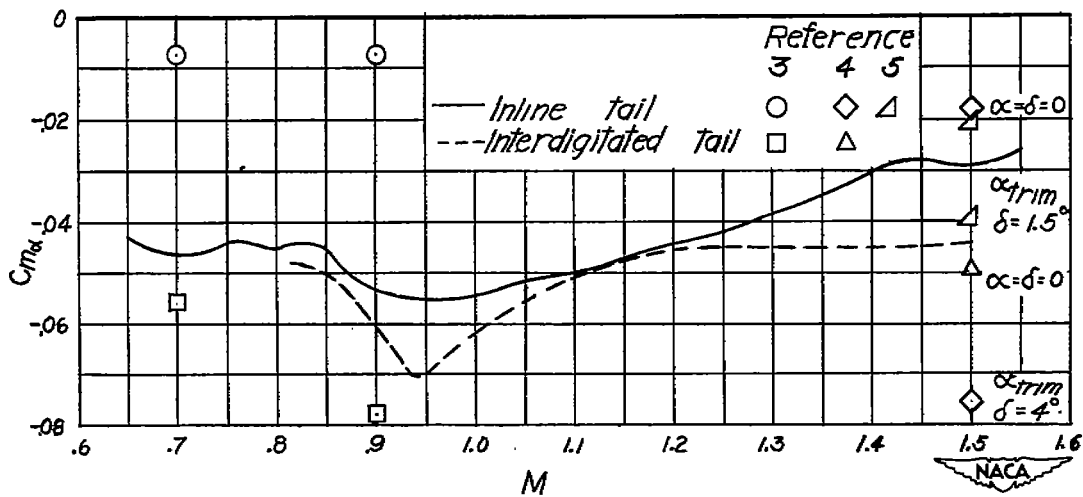


Figure 4.- Variation of static stability with Mach number of inline and interdigitated tail configurations. Center of gravity at 50.8 percent mean aerodynamic chord for both models.

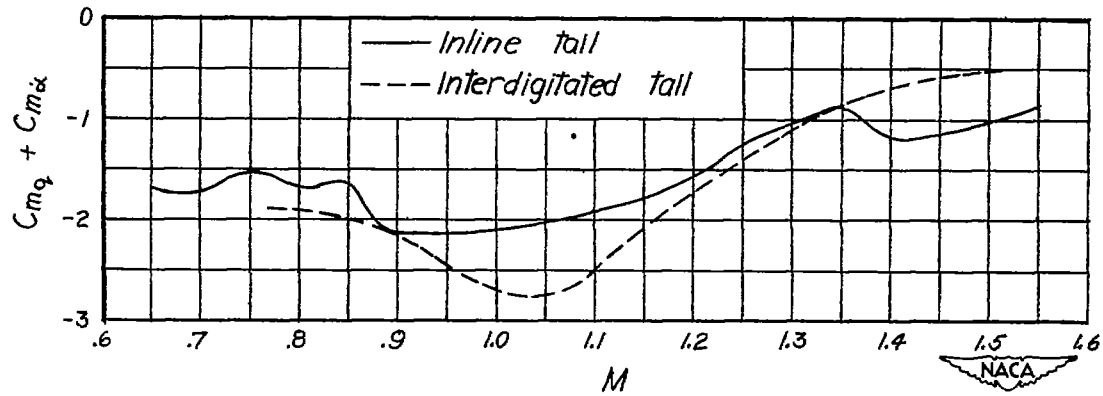


Figure 5.- Variation of damping factor with Mach number for inline and interdigitated tail configurations.

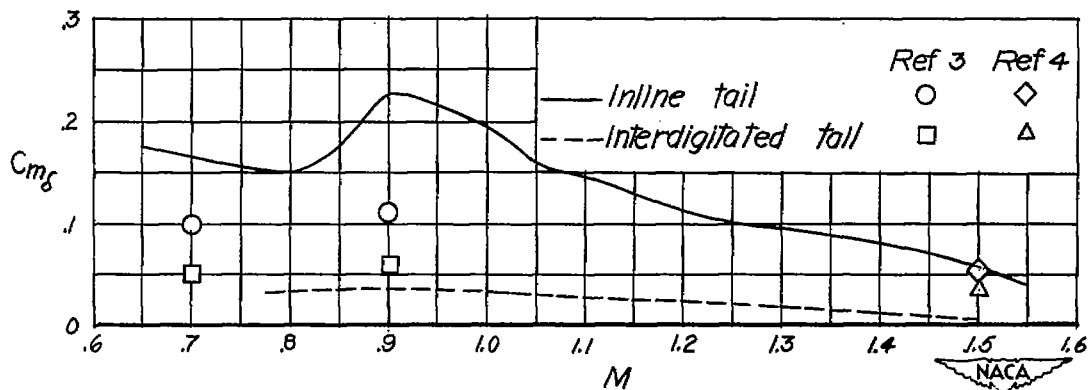


Figure 6.- Variation of $C_{m\delta}$ with Mach number for inline and interdigitated tail configurations.

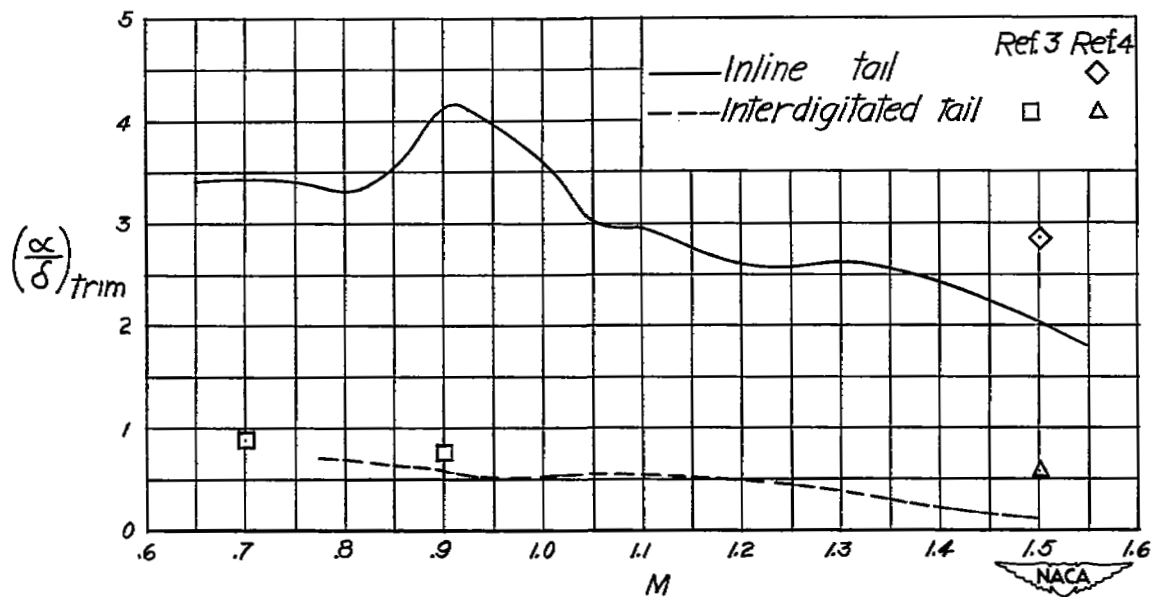


Figure 7.- Variation of $(\alpha/\delta)_{trim}$ with Mach number for inline and interdigitated tail configurations.

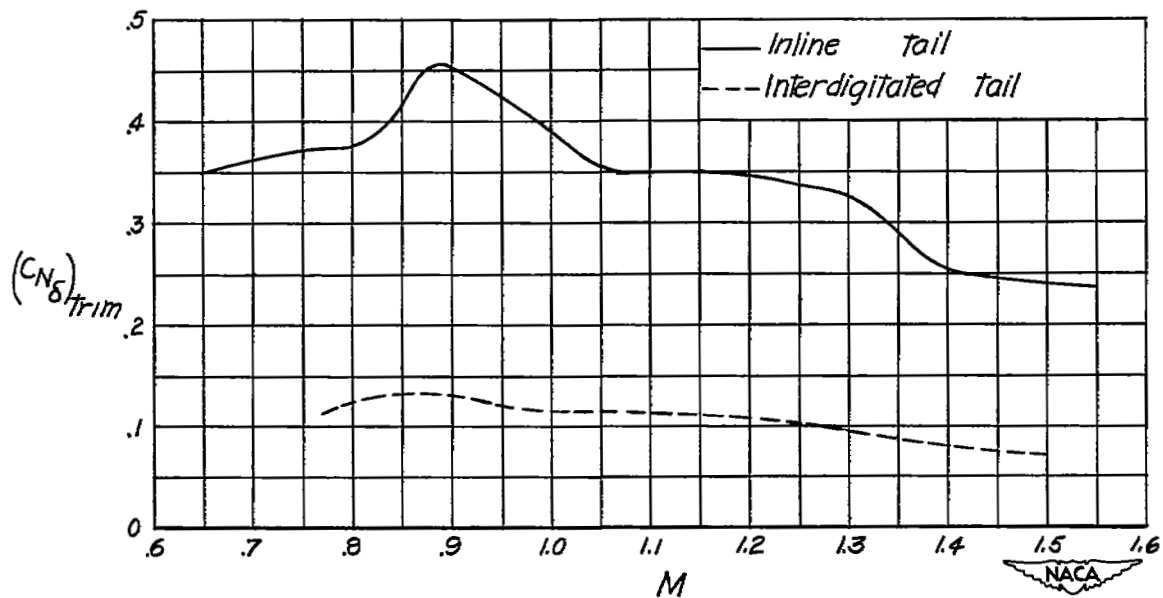
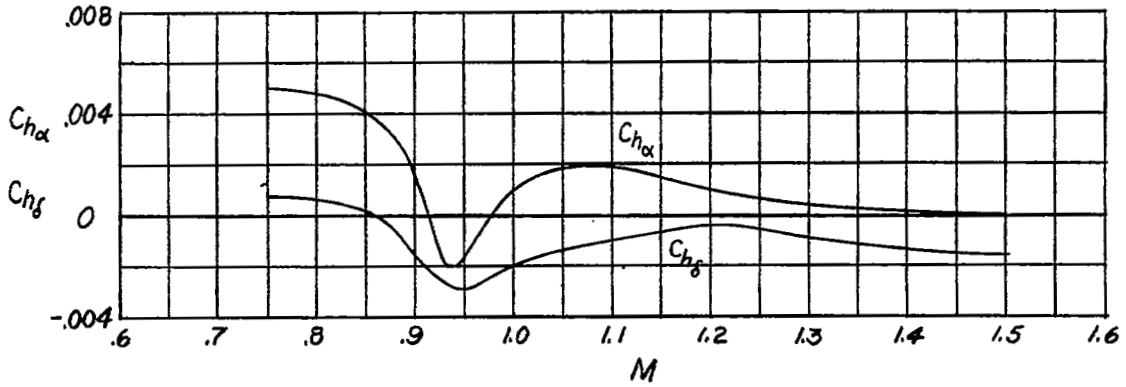
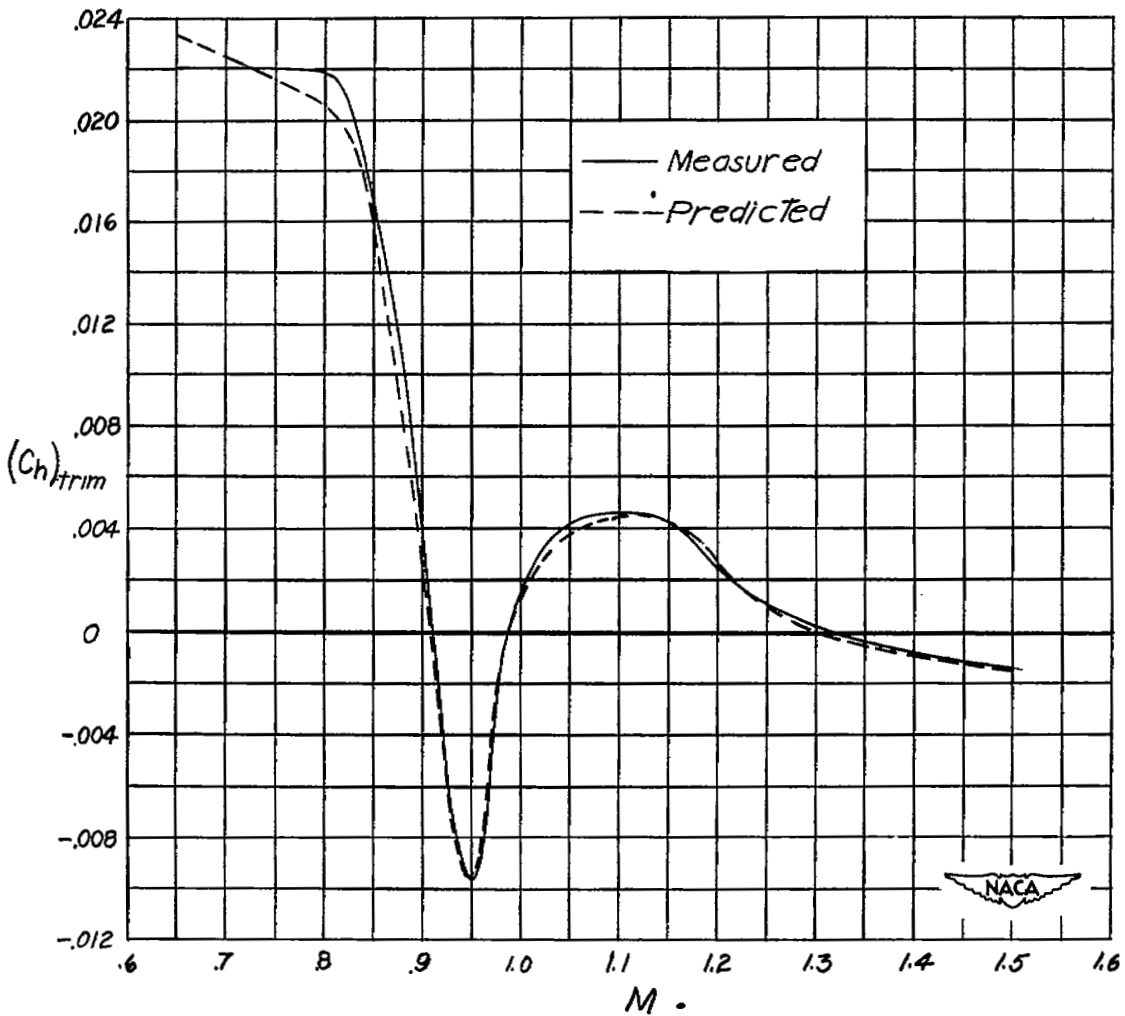


Figure 8.- Variation of $(C_{N\delta})_{trim}$ with Mach number for inline and interdigitated tail configurations.



(a) Hinge-moment variation with Mach number from previous flight test substantiated by current flight test.



(b) Measured and predicted trim hinge moment for inline tail configuration.

Figure 9.- Variation of hinge moments with Mach number.